Hindawi
Advances in Materials Science and Engineering
Volume 2023, Article ID 9870421, 1 page
https://doi.org/10.1155/2023/9870421

Retraction

Retracted: Study on Thermal Performance Measurement and Construction of Passive Exterior Wall with Low Energy: Teaching and Laboratory Building of Shandong Jianzhu University

Advances in Materials Science and Engineering

Received 26 December 2023; Accepted 26 December 2023; Published 29 December 2023

This article has been retracted by Hindawi, as publisher, following an investigation undertaken by the publisher [1]. This investigation has uncovered evidence of systematic manipulation of the publication and peer-review process. We cannot, therefore, vouch for the reliability or integrity of this article.

Please note that this notice is intended solely to alert readers that the peer-review process of this article has been compromised.

Wiley and Hindawi regret that the usual quality checks did not identify these issues before publication and have since put additional measures in place to safeguard research integrity.

We wish to credit our Research Integrity and Research Publishing teams and anonymous and named external researchers and research integrity experts for contributing to this investigation.

The corresponding author, as the representative of all authors, has been given the opportunity to register their agreement or disagreement to this retraction. We have kept a record of any response received.

References

[1] Y. Lan and R. Zou, "Study on Thermal Performance Measurement and Construction of Passive Exterior Wall with Low Energy: Teaching and Laboratory Building of Shandong Jianzhu University," *Advances in Materials Science and Engineering*, vol. 2022, Article ID 3253085, 11 pages, 2022.

Hindawi
Advances in Materials Science and Engineering
Volume 2022, Article ID 3253085, 11 pages
https://doi.org/10.1155/2022/3253085

Research Article

Study on Thermal Performance Measurement and Construction of Passive Exterior Wall with Low Energy: Teaching and Laboratory Building of Shandong Jianzhu University

Yirui Lan[1] **and Ran Zou**[2]

[1]*School of Architecture and Urban Planning, Shandong Jianzhu University, Jinan 250000, Shandong, China*
[2]*School of Management Engineering, Shandong Jianzhu University, Jinan 250000, Shandong, China*

Correspondence should be addressed to Yirui Lan; lanyirui19@sdjzu.edu.cn

Received 22 March 2022; Revised 27 April 2022; Accepted 17 May 2022; Published 3 June 2022

Academic Editor: Palanivel Velmurugan

It can provide theoretical support for the optimal design of low-energy walls by measuring the actual thermal conditions inside the walls of passive low-energy buildings and studying the rationality of the wall structure design. Taking the teaching and laboratory building of Shandong Jianzhu University as an example, this paper explores the method of using temperature and humidity sensor to measure the air temperature and humidity inside the wall to represent the solid temperature and humidity of the wall. Based on the measured data and calculation results, the rationality of the structure of the test external wall is analyzed from four aspects: the performance of insulation, the moisture drain performance of wall, the ability of preventing the penetration of the hot and humid air of the inner wall, and the waterproof performance of the outer wall. Results show that the external wall structure of polystyrene board (200 mm thick) for external insulation and thin plastering has good practical operation effect in three aspects of thermal insulation, internal moisture discharge, and external wall waterproof, which basically meets the design requirements of external wall of passive house in Germany. In terms of moisture protection of the inner wall, the inner wall of cement mortar (15 mm thick) may not be able to effectively prevent the infiltration of indoor hot and humid air. Thus, the insulation layer should be added into the external wall. In addition, the moisture inside the wall is obviously affected by the season. The drain performance of moisture inside the wall mainly occurs in the sweltering heat, and the drain direction is from the indoor side to the outdoor side. In the external insulation structure, there are two layers of graphite polystyrene plate (100 mm thick), and the insulation effect of polystyrene plate near the outdoor side is better than that near the indoor side. The combination of anticrack mortar (5 mm thick) and paint cannot completely prevent the infiltration of rainwater, but the infiltration of rainwater in the wall will be quickly discharged in a short time.

1. Introduction

With the popularization of German passive low-energy buildings in China, the energy-saving technology of high thermal insulation performance, no thermal bridge and high air tightness of exterior wall has been applied in domestic demonstration buildings. The exterior wall construction needs to meet two design goals in order to ensure the energy saving effect of the exterior wall with ultra-low-energy consumption. First, no thermal bridge is required, and the average heat transfer coefficient is less than or equal to 0.15 W/(m^2•K) to effectively block the heat transfer path of the outer wall. This goal has always been the focus of domestic research on energy saving of building envelope. Second, it is necessary to reasonably design the water tightness and air permeability of the inside and outside of the wall to ensure that the inside of the wall is not affected by moisture [1, 2]. This goal has received little attention in academic research and engineering practice. And, today's buildings tend to be low energy and environmentally friendly, so more and more buildings will consider whether the building meets the requirements of low energy consumption.

This study provides a reference scheme for the construction of the external wall without carry and also provides a guarantee for the quality of the wall.

The research of the structure of low-energy insulation wall at home and abroad can be summarized as follows: (1) research institutions used energy consumption calculation software and thermal bridge simulation software to study the structural design of low energy consumption envelope structure and issued authoritative construction standards and Atlas. For example, PHI (Passive House Institute) in Germany has promulgated *Passive Energy Saving Transformation Standard and Passive House Institute Energy Saving Building Standard* [3]. The Center for Science, Technology, and Industrialization Development of the Ministry of Housing and Urban-Rural Development of China has issued the Chinese Standard Atlas, namely, *Passive Low-Energy Buildings—Residential Buildings in Cold Regions* [4]. (2) The researchers used laboratory tests to study the thermal insulation and waterproof vapour insulation performance of building materials. European and American universities and research institutions have carried out a large number of thermal and wet physical property tests of materials. The Fraunhofer Institute of Building Physics in Germany has established a database of physical property parameters of building materials based on the accumulation of long-term test data [5]. Sun et al. studied and tested the thermal and wet physical property parameters of core components of external thermal insulation system, such as concrete, rock wool, EPS, adhesive, and plaster [6]. Yu carried out in-depth theoretical and experimental research on the thermal performance of wall building materials based on temperature and humidity [7]. (3) The researchers used numerical simulation to study the influence of wall construction practices or new building materials on wall moisture and heat performance. Jia simulated and analyzed the influence of polystyrene board and gap between them of composite insulation wall on the humid and hot state of the wall [8]. Chang et al. simulated the moisture and heat properties of cross-laminated wood and analyzed its moisture risk in 20 cities in South Korea [9]. Park et al. simulated the humidity and heat performance of walls using functional gypsum board (with porous materials and PCM added into the board) [10]. Havinga and Schellen simulated and analyzed the design factors affecting mold and condensation inside the wall during the energy-saving transformation of prefabricated buildings with internal thermal insulation [11]. (4) The temperature and humidity change inside the wall is measured to study the thermal performance of a component or a structural hierarchy of the wall quantitatively. Xue measured and compared the relative humidity changes of concrete base of EPS external insulation wall in Harbin at different time after completion and proposed that indoor and outdoor environment was the main factor affecting the humidity state of concrete layer [12]. Xia et al. measured the change of relative humidity in the base wall and insulation layer after the completion of two kinds of insulation walls in Harbin and pointed out that the increase of humidity would not affect the insulation performance of extruded polystyrene board [13, 14]. McClung et al. measured the humidity and mold inside 16 kinds of walls composed of cross-laminate and analyzed the drying process of cross-laminate [15]. To sum up, the study of moisture and heat of building wall is the important and difficult point of the study of thermal insulation wall structure. The domestic construction field does not pay enough attention to the water vapor permeability coefficient of building materials and lacks long-term measurement and tracking of humidity and heat parameters of walls with high thermal insulation and low energy consumption. Thus, it is impossible to determine whether the completed exterior walls with low energy consumption can effectively reach the water vapor penetration and isolation requirements of the wall.

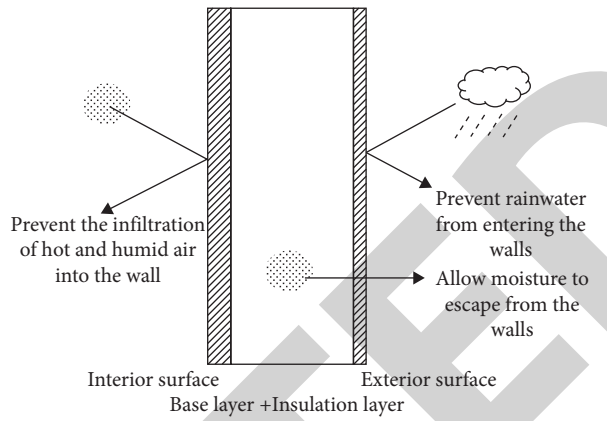

Figure 1: Design principles for water tightness and air permeability of low-energy exterior wall finishes.

Therefore, taking the passive low-energy building demonstration project of Shandong Jianhua University as an example, this study used temperature and humidity sensors embedded in the wall to measure the temperature and humidity data at different locations in the external wall for a long time, in order to analyze the change rule of temperature and humidity inside the wall and to study the rationality of the wall construction, which can provide data support for the relevant researches. In addition, this study provides a reference scheme for the construction and inspection of building exterior walls.

2. Experimental Test of Thermal Performance

2.1. The Test Wall. In the design and construction process of passive low-energy buildings in China, the design principles should be followed as follows: the water vapor penetration resistance of the interior decorative layer is large, which prevents the indoor hot and humid air from penetrating into the wall in winter, while the high water tightness and low resistance of water vapor penetration of the exterior veneering layer prevent outdoor rainwater from entering into the wall and allow moisture to escape from the wall. The design principle of watertight and breathable design of low-energy exterior wall finishes is to reflect the performance of the exterior wall through the watertight and breathable condition of the exterior wall. The design principle of water tightness and air permeability of low-energy exterior wall finishes is shown in Figure 1.

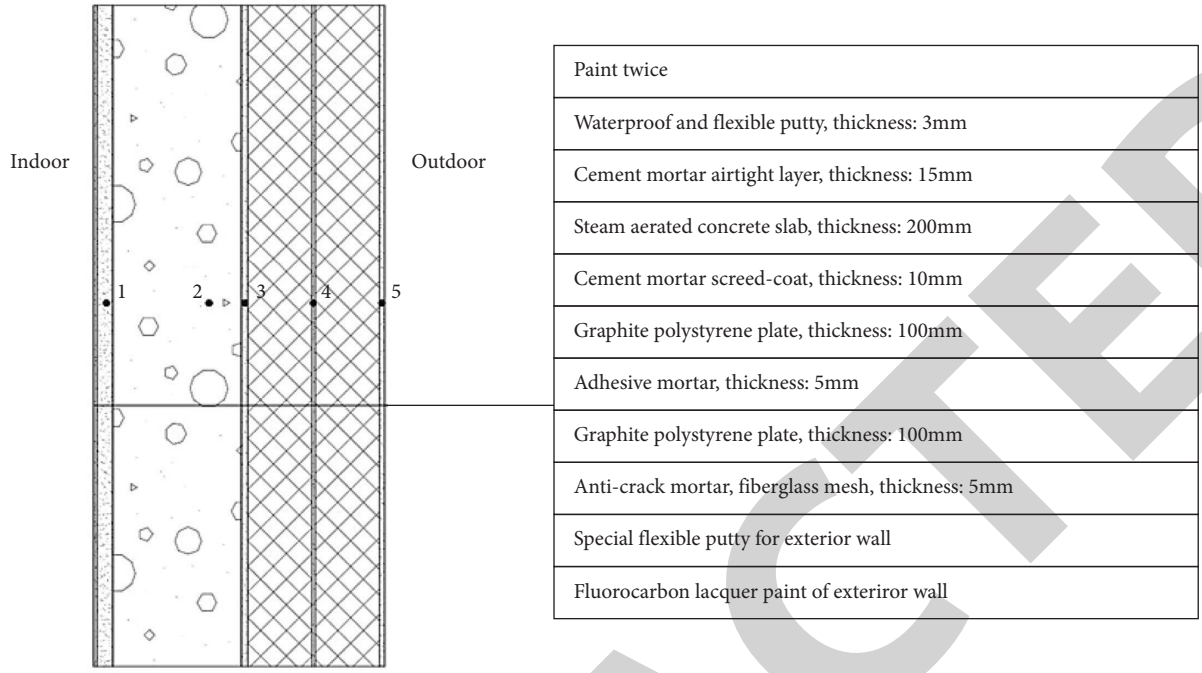

Figure 2: The structure of the test wall and the location of temperature and humidity measurement points in the wall. (1–5 represent the locations of temperature and humidity measurement points).

The Teaching and Laboratory Building of Shandong Jianzhu University, located in Jinan City, was completed in March 2017. It is a Sino-German cooperative demonstration project of passive low-energy buildings of the Ministry of Housing and Urban-Rural Development and the first batch of low-energy building demonstration project in Shandong Province. The main building has a total of 6 floors, with a total building height of 23.96 m and a total construction area of 9696.3 m^2. The exterior wall of the project was designed according to the principles shown in Figure 1, with a heat transfer coefficient of 0.14 W/(m^2•K). The heat transfer coefficient K of the wall is the characteristic of the wall (including all structural levels) under stable heat transfer conditions, when the air on both sides of the wall. When the temperature difference is 1 K (1°C), the heat transferred through the unit square meter of wall area per unit time. The structural layers are shown in Figure 2, and the relevant physical properties of the building materials of the exterior wall are tested and shown in Table 1.

2.2. The Location of Measurement Points. The temperature and humidity sensors were located in three types of positions in this experiment according to the structural hierarchy of the test wall and the physical properties of the building materials. The first type is the position where the wall is in contact with the indoor and outdoor environment, such as points 1 and 5 shown in Figure 2. The second type is the position between two adjacent main structural layers, such as points 3 and 4 shown in Figure 2. The third type is the interior of building materials with high water vapor permeability coefficient, such as point 2 shown in Figure 2.

In this study, temperature and humidity sensors were placed inside the test wall of the building in the east, south, west, and north directions, respectively, according to locations of the measurement points shown in Figure 2, and a total of 4 sets of temperature and humidity measuring equipment were prepared in order to collect related data.

2.3. Experiment Equipment. The experiment equipment adopts temperature and humidity integrated sensor (Visara HMP100) and plastic protective tube (19266HM). The shape and size of HMP100 and plastic protective tube are shown in Figure 3. Referring to "*Visala Structure Humidity Test Kit*," the air temperature and humidity in the enclosed space inside the building component were measured to represent the temperature and humidity data of a test position inside the wall. HMP100 has two sensor elements: the temperature sensor (PT100) and the thin-film capacitive humidity sensor element, which is covered with a plastic filter (including a filter plastic grid and a filter membrane with a porosity of 0.2 m, as shown in Figure 3(a)) to protect sensor components and filter dust. The plastic filter mainly filters the impurities generated during measurement. The above components constitute an effective test cavity to ensure the normal operation of the sensor. The temperature measurement range of the sensor is −40 to 80°C, and the relationship between temperature and accuracy is as follows: accuracy ±0.2°C (temperature in the range of 0–40°C) and accuracy ±0.4°C (temperature in the range of −40 to 0°C). The relative humidity measurement range of the sensor is 0–100%, and the relationship between temperature, relative humidity and accuracy is as follows: accuracy ±1.5% (temperature in the range of 0–40°C, humidity in the range of 0–90%) and accuracy ±3.0% (temperature in the range of −40 to 0°C, humidity in the range of 0–90%). In order to

Table 1: Physical property parameters of building materials for the test external wall.

ID	Structural layer	Heat conductivity coefficient ($w \cdot m^{-1} \cdot K^{-1}$)	Thickness (mm)	Water vapor penetration coefficient, μ ($ng \cdot Pa^{-1} m^{-1} \cdot s^{-1}$)	Sensor ID
1	Coating material of interior wall				
2	M7.5 cement mortar	0.93	15	5.8	1
3	Steam aerated concrete slab	0.146	200	27.7	2
4	M7.5 cement mortar	0.93	10	5.8	3
5	Graphite polystyrene plate	0.032	100	4.5	
6	Adhesive mortar	0.93	5	5.8	4
7	Graphite polystyrene plate	0.032	100	4.5	
8	Anticrack mortar	0.93	5	5.8	5
9	Fluorocarbon lacquer paint of exterior wall			0.1 mL*	

*According to the test method of JG/T210-2007 "*Primer for Building Internal and External Walls*," the water permeability test result of the alkali resistant sealing primer for the external wall coating of this project is 0.1 ml, and the water resistance test result is 96 h without abnormality. *Water vapor permeability coefficient refers to the water vapor partial pressure difference on both sides of a material with a thickness of 1 m under stable penetration conditions of 1 Pa, within 1 hour (the amount of water vapour that penetrates through an area of 1 square meter).

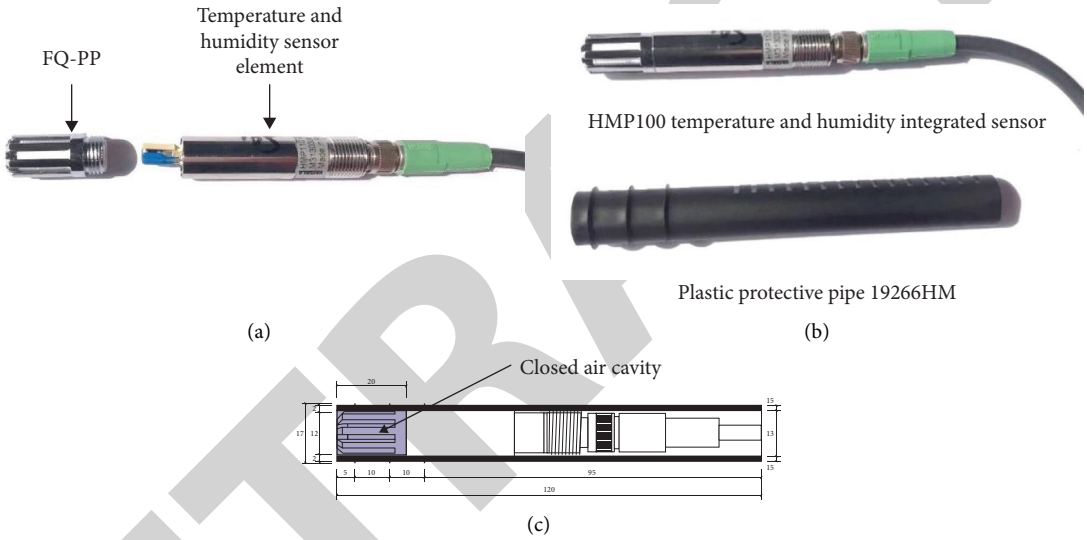

Figure 3: The shape and size of the temperature and humidity measurement equipment inside the wall. (a) FQ-PP (built-in filter membrane with 0.2 μm pore), temperature, and humidity sensor element. (b) HMP100 temperature and humidity integrated sensor, plastic protective pipe 19266HM. (c) HMP100 temperature and humidity integrated sensor, plastic protective pipe 19266HM (after assembly).

measure the internal temperature and humidity of solid materials, Visala developed a plastic pipe 19266HM for the HMP100 sensor to protect it and seal the air inside the plastic filter to ensure that the sensor can measure the temperature and humidity of the test position inside the wall (Figure 3(c)).

2.4. The Installation Method of Experiment Equipment. The size of the experiment equipment after assembly is large (diameter is 17 mm, and length is 120 mm). In this study, the thickness and construction technology of the wall structure layer are combined in the construction process, and two installation methods are used: (1) applied to the external wall base (point 2); (2) applied to exterior mortar layer (points 1, 3, 4, and 5).

(1) Installation method for sensors inside autoclaved aerated concrete slabs (point 2, Figure 4)

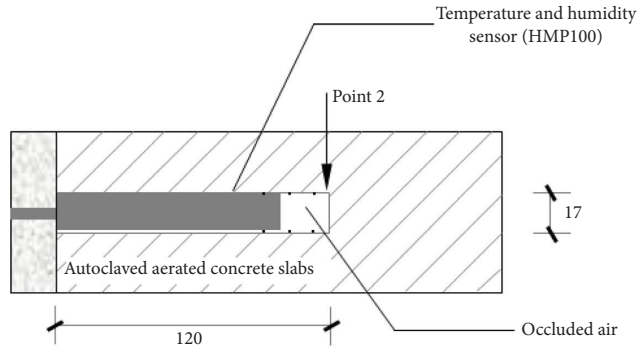

Figure 4: Installation method for sensors inside autoclaved aerated concrete slabs (/mm).

① After the autoclaved aerated concrete slabs are installed in place, a hole is drilled in the slabs from the inside to the outside perpendicular to the wall, with the diameter of 17 mm and the depth of 120 m

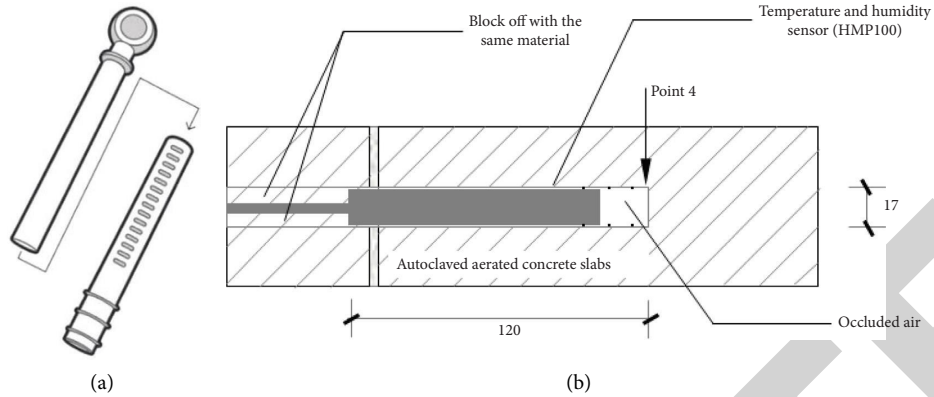

Figure 5: Installation method for sensors inside external wall mortar layer. (a) Embolize the long rubber into the plastic pipe. (b) Detailed construction drawing of sensor inside the mortar layer (/mm, point 4).

② Use a high-pressure dust blower to clean the inside of the hole
③ Use a rubber hammer to knock the plastic pipe into the hole
④ Inserted the HMP100 sensor into the plastic pipe, and then the construction of the airtight layer of the cement mortar of indoor side is carried out

(2) Installation method for sensors inside external wall mortar layer (point 4, Figure 5)

① After the construction of the first graphite polystyrene plate on the left of point 4 is completed, a hole is drilled from the outside to the inside perpendicular to the wall with the diameter of 17 mm, and the depth runs through the first graphite polystyrene plate and the autoclaved aerated concrete strip.
② Embolize the long rubber into the plastic pipe, and knock the plastic pipe into the hole with a rubber hammer. The bottom of the plastic casing is located at the interior side of the thickness range of the bonding mortar layer.
③ The second layer of graphite polystyrene plate is constructed by the way of full adhesion. The long rubber plug can prevent the mortar from entering the plastic pipe. After the mortar solidifies, we can pull out the long rubber plug from the plastic pipe and clean the inside of the plastic pipe with a high-pressure dust gun.
④ Insert the HMP100 sensor is into the plastic tube, and seal the hole with the same material.

The installation method for sensors located in the positions of points 1, 3, and 5 are the same as point 4.

2.5. Experiment Process. 20 temperature and humidity sensors were embedded inside the external wall in the east, south, west, and north directions with the installation methods above, and temperature and humidity sensors were installed in the indoor and outside of the wall, respectively. The temperature t and relative humidity φ of the indoor and outside air of the wall and the wet air in the inner cavity of the wall were measured. The measured data were recorded every 30 min and then transmitted to the data platform through the network cable for storage. The whole test system has been running since February 2018. The embedded sensors in the east, south, and north external walls can work normally, while the embedded sensors in the west external wall failed to work normally.

3. Data Process

3.1. Calculation of Experimental Data. The state parameters of wet air include total pressure B, specific enthalpy H, moisture content d, temperature t, relative humidity φ, and water vapor partial pressure P_v. The state of wet air can be determined by three independent parameters including total pressure B, temperature t, and relative humidity φ. The temperature t of the wet air in the cavity measured by the sensor can be considered as the solid temperature of the wall at the location of the cavity. The material of the test wall is porous, and the cavity in the wall is connected with the atmosphere through the pores of the building's internal and external surface materials. Therefore, it is approximately considered that the total atmospheric pressure B in the cavity is unchanged and can be regarded as a constant 101.325 kPa.

The system can automatically record the temperature t_{ij} and relative humidity φ_{ij} of the air in the cavity at a certain time j at the test position i. According to the function relationship between the main parameters of wet air, the moisture content d_{ij} of the air in the cavity at a certain time j at the test position i can be calculated. The specific calculation formulas are as follows:

$$d_{ij} = 622\frac{P_{vij}}{B - P_{vij}}, \qquad P_{vij} = P_{v.b} \cdot \varphi_{ij}, \tag{1}$$

where d_{ij} is the moisture content of test position i at a certain time j, and its unit is g/kg; P_{vij} is the partial pressure of water vapor at the test position i at a certain time j, and its unit is Pa; $P_{v.b}$ is the saturated water vapor pressure at the

temperature t_{ij} at the test position i at a certain time j, and its unit is Pa; and φ_{ij} is the relative humidity of test position i at a certain time j.

It should be noted that φ_{ij} and d_{ij} are the relative humidity and moisture content of the air in the cavity at test position i, rather than the humidity status of the solid wall at test position i. Therefore, the relative humidity and the moisture content of the air in the cavity obtained by the test system are used to represent the humidity status of the solid wall at the location of the cavity in this paper.

3.2. The Analysis Methods of Experimental Data. Based on the measured data and calculation results, the rationality of the structure of the test external wall is analyzed from four aspects: the performance of insulation, the moisture drain performance of wall, the ability of preventing the penetration of the hot and humid air of the inner wall, and the waterproof performance of the outer wall. The reason for the analysis from these four aspects is mainly because these four aspects cover all aspects of the outer wall:

(1) The performance of insulation: in order to avoid the interference of direct sunlight, this experiment selects the measured temperature data of the north wall on the coldest and hottest day during the test period to analyze the thermal insulation performance of the wall.

(2) The moisture drain performance of wall: the wall drains moisture outdoors in summer and absorbs moisture indoors in winter. In summer, the internal moisture is vaporized by sunlight and expelled. The annual measured humidity data inside the south-facing wall were selected to analyze the moisture drain performance of wall.

(3) The ability of preventing the penetration of the hot and humid air of the inner wall: in winter, the indoor hot and humid air will permeate into the wall. The measured humidity data of the wall during the heating of the east, south and north walls were selected to analyze the moisture-proof performance of the inner wall surface.

(4) The waterproof performance of the outer wall: the wind direction in Jinan city is changeable, and the east and southeast wind are the majority in the rainy season. Thus, the waterproof performance of the east wall and the outer wall is the most unfavorable. The measured humidity data of the east wall before and after the precipitation was selected to analyze the waterproof performance of the outer wall.

This study selected the whole year measured data from March 26, 2018, to March 26, 2019, for analysis. The working condition of one day between two precipitation periods from April 7, 2019, to April 13, 2019, can clearly reflect the waterproof performance of the outer wall surface. Therefore, the measured data in April 2019 was selected for the analysis of the waterproof performance of the outer wall surface.

3.2.1. The Performance of Insulation of Wall. The thermal insulation performance of the structural layer of outer wall can be approximately represented by the temperature difference between the test positions on both sides of the structural layer. The smaller the temperature difference is, the better the thermal insulation performance is. The temperature difference between test position i and $i+1$ at a certain time j is calculated by

$$\Delta t_{(i+1)ij} = \left| t_{(i+1)j} - t_{ij} \right|, \tag{2}$$

where $\Delta t_{(i+1)ij}$ is the absolute value of the temperature difference between test position i and test position $i+1$ at a certain time j, and the unit is °C; t_{ij} and $t_{(i+1)j}$ are the temperature values of test position i and test position $i+1$ at a certain time j, and the unit is °C; i is the test position inside the wall, with values of 1, 3, 4, 5; j is the hour of the day, with values of 0, 1, 2, . . ., 23. The test wall is composed of thick aerated concrete slabs with the thickness of 200 mm, thick inner graphite polystyrene plate with the thickness of 100 mm, and thick outer graphite polystyrene plate with the thickness of 100 mm. In Figure 2, test positions 1, 3, 4, and 5 are, respectively, distributed on both sides of the structure layers. The thermal insulation performance of thick aerated concrete strip (200 mm), thick inner graphite polystyrene plate (100 mm), and thick outer graphite polystyrene plate (100 mm) can be characterized by $\Delta t_{31j}, \Delta t_{43j}$, and Δt_{54j}, respectively.

The steps of thermal insulation analysis of the wall are as follows:

(1) Take the position of the test point as the abscissa and the internal temperature of the wall as the ordinate and draw the temperature points of test position 1, 3, 4, and 5 at time j on the coldest day during the test period. Then, connect the temperature points into a broken line. In the same way, draw the temperature polylines for 24 hours of the day.

(2) Analyze the 24 temperature lines above and select the broken lines at some time when the temperature difference between inside (point 1) and outside (point 5) wall is large and the steady-state heat transfer approaches one dimension. Calculate $\Delta t_{31j}, \Delta t_{43j}$, and Δt_{54j} of those broken lines and calculate the average values ($\overline{\Delta t}_{31H}, \overline{\Delta t}_{43H}$, and $\overline{\Delta t}_{54H}$) as the evaluation basis of the heat preservation performance of the wall in winter.

(3) The actual insulation effect of aerated concrete strip, inner graphite polystyrene plate, and outer graphite polystyrene plate was evaluated by comparing the relationship between the average values ($\overline{\Delta t}_{31H}$, $\overline{\Delta t}_{43H}$, and $\overline{\Delta t}_{54H}$) and the heat transfer coefficients (K_{31}, K_{43}, and K_{54}) of the corresponding structure layers.

(4) The average values ($\overline{\Delta t}_{31H}, \overline{\Delta t}_{43H}$, and $\overline{\Delta t}_{54H}$) of the hottest days during the test period were calculated to evaluate the actual thermal insulation performance of the main structural layers in summer with the same method.

Table 2: The water vapor permeability resistance at the test location of the exterior wall.

Test location	Water vapor permeability resistance, H ($Pa \cdot m^2 \cdot s \cdot \mu g^{-1}$)	
	Indoor side	Outdoor side
1	2.59	55.11
2	6.92	50.78
3	9.81	47.89
4	33.75	23.95
5	56.84	0.86

3.2.2. The Moisture Drain Performance of Wall. Calculate the water vapor permeability resistance of the indoor and outdoor side of the test location based on the thickness of the building structure layers, the position of temperature and humidity sensor, and the water vapor permeability coefficient μ of the building material. The calculation results are shown in Table 2.

In the process of exterior wall construction, the residual moisture is discharged to the indoor and outdoor, and it is difficult to discharge moisture at test position 2, 3, and 4. Therefore, the average daily moisture content $\overline{d}_i$ of test position 2, 3, and 4 was calculated, respectively, in this study to evaluate the residual moisture drain performance inside the test wall. The calculation formula of the average moisture content is as follows:

$$\overline{d}_i = \frac{\sum_{j=0}^{n} d_{ij}}{24}, \quad (3)$$

where $\overline{d}_i$ is the average daily moisture content at test position i, and the unit is g/kg, and d_{ij} is the moisture content at a certain time j in position i, the unit is g/kg.

3.2.3. The Waterproof Performance of the Outer Wall. Therefore, study the daily precipitation before and after the precipitation process and the average daily moisture content ($\overline{d}_i$) at test position 5, 4, and 3 during the period to analyze the effect of precipitation on the moisture content of the outdoor side and wall and evaluate the waterproof performance of the outer wall.

3.2.4. The Ability of Preventing the Penetration of the Hot and Humid Air of the Inner Wall. The indoor temperature and humidity of the building in winter are higher than the outdoor environment, and the water vapor flows to the outdoor through the envelope structure, which may result in the problem of moisture accumulation inside the wall. In order to ensure the durability and thermal insulation of materials, GB 50176-2016 "Code for Civil Building Thermal Design" stipulates that the increment of mass humidity of the insulation materials ($\Delta\omega$) shall not exceed a certain limit after a heating period. Thus, the moisture in the insulation materials can gradually distribute after the heating period, rather than accumulate inside year by year. The limits of $\Delta\omega$ are shown in Table 3.

Table 3: The allowed increment of mass humidity of the envelope insulation material during heating period.

Insulation material	The allowed increment of mass humidity $[\Delta\omega]$ (%)
Porous concrete (foamed concrete, aerated concrete, etc.) ($\rho_0 = 500 \sim 700\ kg/m^3$)	4
Model polystyrene foam	15

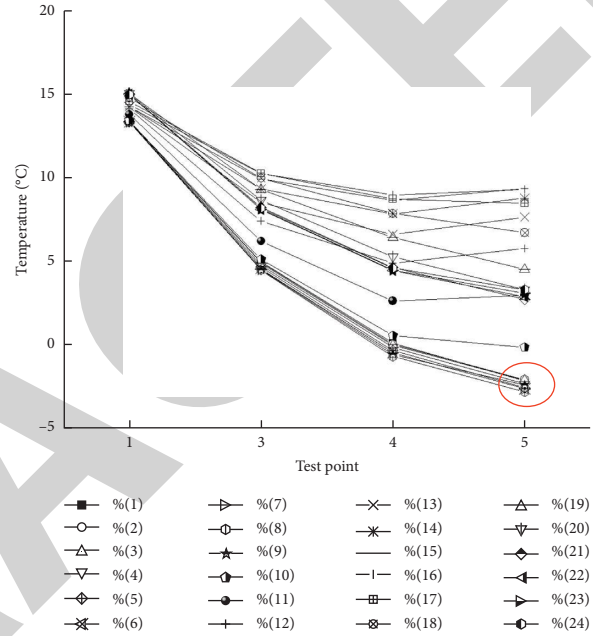

Figure 6: Temperature curve on the hour of the indoor side of the north-facing wall on January 13 (the coldest day during the test period).

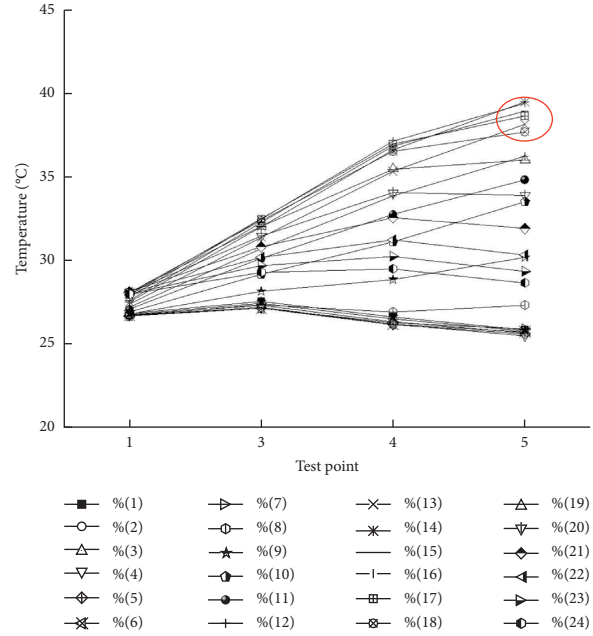

Figure 7: Temperature curve on the hour of the indoor side of the north-facing wall on July 11 (the hottest day during the test period).

Table 4: Thermal insulation performance of main structural layers of exterior wall.

Structural hierarchy	Test point	Thermal resistance, R ($m^2 \cdot k \cdot w^{-1}$)	Heat insulation performance, $\overline{\Delta t}_H$ (°C)	Insulation performance, $\overline{\Delta t}_C$ (°C)	Heat insulation performance of each unit of thermal resistance, $\overline{\Delta t}_H/R$ (°C)	Insulation performance of each unit of thermal resistance, $\overline{\Delta t}_C/R$ (°C)
Aerated concrete slabs	Point 1, 3	14.29	8.66	4.58	0.61	0.32
Inner graphite polystyrene plate	Point 3, 4	33.33	4.97	4.58	0.15	0.14
Outer graphite polystyrene plate	Point 4, 5	33.33	2.13	2.2	0.06	0.07

The increment of moisture content before and after the heating period can be represented by the increment of mass humidity of aerated concrete slats and graphite polystyrene slats inside the wall after the heating period. The calculation formula is shown as follows:

$$\Delta\omega_i = \frac{\left(\overline{d}_{iHE} - \overline{d}_{iHS}\right)}{\overline{d}_{iHS}} \times 100\%, \quad (4)$$

where $\Delta\omega_i$ is the increment of mass humidity of material at test position i after the heating period; $\overline{d}_{iHS}$ and $\overline{d}_{iHE}$ are the average daily moisture content of test position i at the beginning and end of the heating period, respectively, and the unit is g/kg. The actual heating period in Jinan begins on November 15 each year and ends on March 15 of the following year. Thus, $\overline{d}_{iHS}$ and $\overline{d}_{iHE}$ are the average moisture content of test position i on November 15 of the current year and March 15 of the following year.

The necessary and sufficient condition to judge that the internal surface of the wall has good performance in preventing the infiltration of hot and humid air is $\Delta\omega_i \leq [\Delta\omega]$. Based on the judgment, the ability of preventing the penetration of the hot and humid air of the test inner wall can be evaluated.

4. Results

4.1. The Performance of Insulation of Wall. The coldest and hottest days of the year during the test period were January 13 and July 11, 2018. The temperature curves of the north-facing exterior wall on the hour are shown in Figures 6 and 7, respectively. It can be seen from Figure 6 that the temperature at different hours showed a trend of gradual decrease from indoor to outdoor (test point 1 to test point 5) in the coldest day of the year during the test period. During the coldest day, the temperature of the inner wall fluctuates in the range of 13.3~15.0°C, and the fluctuation range is obviously smaller than that of the outer wall (−2.8~9.3°C), which indicates that the wall has good thermal insulation performance on the coldest day and can keep the indoor temperature relatively stable without being affected by the outdoor cold air. At the same time, it can be seen from Figure 7 that the temperature at different hours from indoor to outdoor (test point 1 to test point 5) mostly showed a gradually rising trend in the hottest day of the year during the test period. During the hottest day, the temperature of the inner wall fluctuates in the range of 26.7~28.1°C, and the fluctuation range is obviously smaller than that of the outer wall (25.5~39.5°C), which indicates that the inner wall has good thermal insulation performance and can keep the indoor temperature relatively stable without being affected by the outdoor warm air.

The points circled with red circle in Figure 6 shows the temperature values from 0 to 8 o 'clock on January 13, and the points circled with red circle in Figure 7 shows the temperature values from 13 to 16 o 'clock on July 11. During these two periods, the heat transfer inside the wall is close to one-dimensional steady heat transfer, and the average temperature difference of the main structural layers is shown in Table 4. The temperature difference between the two sides of the aerated concrete strip (200 mm) was significantly higher than that of the inner graphite polystyrene plate (100 mm) and the outer graphite polystyrene plate (100 mm), and the heat insulation performance of each unit of thermal resistance was 0.61°C, 0.15°C, and 0.06°C, respectively. The insulation performance was 0.32°C, 0.14°C, and 0.07°C, respectively, indicating that the thermal insulation performance of 100 mm graphite polystyrene plate in summer and winter was better than that of 200 mm aerated concrete strip slab with twice the thickness of it. At the same time, due to the complexity of the actual heat transfer process, the insulation performance of the graphite polystyrene plate with the same thickness applied on the inside and outside of the external wall is also different to some extent. As can be seen from Table 4, the insulation performance of the graphite polystyrene plate with the same thickness on the outside of the external wall is about 2 times better than that on the inside of the external wall.

4.2. The Moisture Drain Performance of Wall. The average daily moisture content in one year (from March 26, 2018 to March 26, 2019) of test point 2, 3, and 4 inside the east wall was calculated based on (3). The results are shown in Figure 8. The moisture content of steam pressurized concrete slab inside the east wall (test point 2) is the largest throughout the year; the moisture content of the inner graphite polystyrene plate (test point 3) is next, and the outer

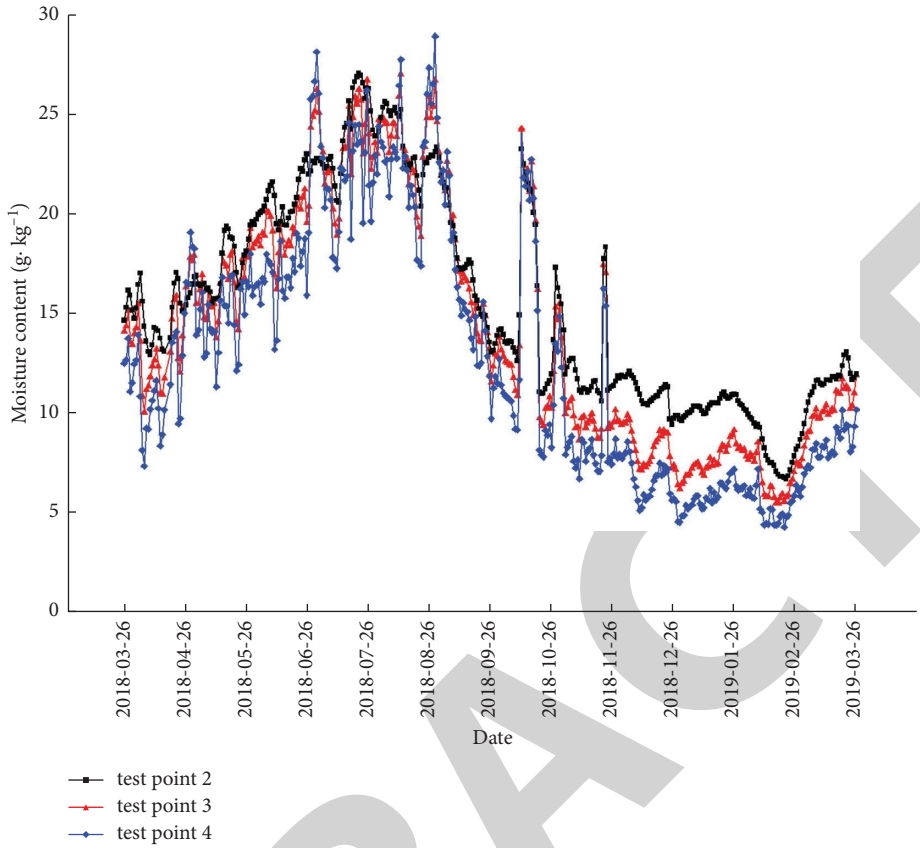

Figure 8: The curve of average daily moisture content inside the east wall.

graphite polystyrene plate is the smallest. In addition, the water vapor permeability resistance of test point 2 on the outdoor side is higher than test points 3 and 4 (see Table 2). It can be seen that the moisture inside the wall is mainly discharged to the outside wall.

The moisture content inside the east wall decreases in summer and autumn, especially from August to October with high temperature. On the contrary, the moisture content rises in spring and winter. The moisture content of test points 2, 3, and 4 inside the wall decreased little after one year, with a decrease of 18.4%, 15.6%, and 18.4%, respectively. In Figure 8, the moisture content of point A and B increased sharply during the test time. After investigation, it was found that points A and B were all in case of heavy rain, and the moisture content inside the wall was changed due to rainwater penetration.

4.3. The Waterproof Performance of the Outer Wall. There was significant precipitation on April 9 and April 11, 2019. The moisture content and precipitation at test points 3, 4, and 5 inside the east wall from April 7, 2019, to April 13 were selected to carry out waterproof analysis on the outer wall. The measured data are shown in Figure 9. It can be seen from Figure 9 that the precipitation on April 9 and 11 caused the moisture content of the outer wall (test point 5) to increase significantly on April 10 and 12, and the rainwater that penetrated into the outer wall was then discharged rapidly.

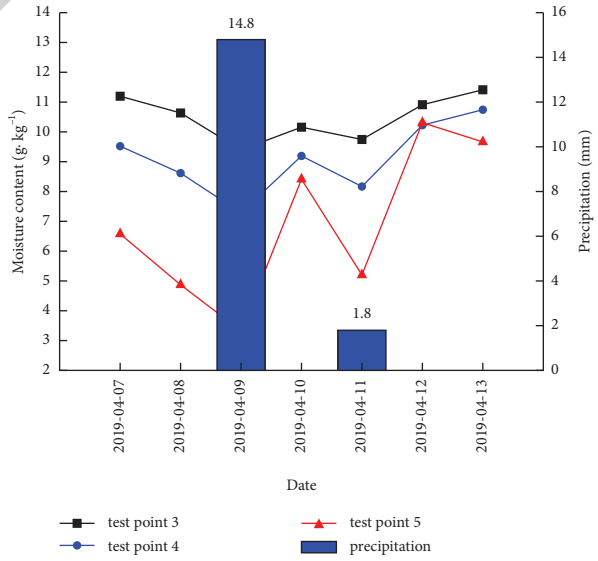

Figure 9: Average daily moisture content and precipitation inside the east wall.

The moisture content of the outer wall (test point 5) began to decrease on April 11 and 13. The moisture content of the graphite polystyrene plate (test position 4, 3) fluctuated in the same way as that of the outer surface of the external wall, but the fluctuation range was reduced. The measured data show that the outer surface of the external wall cannot

Table 5: Increment of mass humidity of insulation material inside the external wall after heating period.

Structural hierarchy	Test point	Heating period in 2018, $\Delta\omega_i$			The allowed increment of mass humidity $[\Delta\omega]$ (%)
		East wall	South wall	North wall	
Aerated concrete slabs	Point 2	6.43	14.9	1.99	4
Graphite polystyrene plate	Point 4	3.66	17.73	−2.39	15

completely prevent the infiltration of rainwater, but the influence time of rainwater on moisture content inside external wall is short since the rainwater that penetrates into the wall will be discharged quickly.

4.4. The Ability of Preventing the Penetration of the Hot and Humid Air of the Inner Wall. The heating period in winter in Jinan is from November 15 to March 15 of the next year. Therefore, the increments of mass humidity of building materials at the test point 2 and 4 of the east, south, and north exterior walls after the heating season in 2018 were calculated, respectively, based on (4). The calculation results are shown in Table 5. The increments of mass humidity of aerated concrete slabs on the east and south wall is 6.43% and 14.9%, respectively, after the heating season in 2018, exceeding the allowable increment of mass humidity of aerated concrete slabs by 4%. The increment of mass humidity of graphite polystyrene plate on the south wall is 17.73%, exceeding the allowable increment of mass humidity of graphite polystyrene plate by 15%. The infiltration of indoor hot and humid air in winter is not the only reason for the increase of moisture content inside the wall. Through the data analysis of one heating season, it can only be determined that the infiltration of indoor hot and humid air cannot be effectively prevented by the inner wall surface with the cement mortar airtight layer (15 mm) in this project. The exact conclusion needs the comprehensive comparative analysis of the data of multiple heating periods.

5. Conclusion

In this paper, the thermal performance of the exterior wall of the teaching and laboratory building of Shandong Jianzhu University was measured and the structural rationality was studied. The main conclusions are as follows:

(1) The temperature and humidity sensors were used to continuously measure the temperature and humidity of the air inside the cavity of the wall, which can be used to represent the temperature and humidity of the solid wall at the position of the cavity. In order to ensure that the cavity data can accurately reflect the temperature and humidity of the wall, the installation design and construction process of the sensor must meet the requirements of air sealing of the cavity in the wall and accurate installation position of the sensor.

(2) The external wall structure of polystyrene board (200 mm thick) for external insulation and thin plastering has good practical operation effect in three aspects of thermal insulation, internal moisture discharge, and external wall waterproof, which basically meets the design requirements of external wall of passive house in Germany. In terms of moisture protection of the inner wall, the inner wall of cement mortar (15 mm thick) may not be able to effectively prevent the infiltration of indoor hot and humid air. Thus, the insulation layer should be added into the external wall.

(3) The moisture inside the wall is obviously affected by the season. The moisture content increases in spring and winter and decreases in summer and autumn. The drain performance of moisture inside the wall mainly occurs in the sweltering heat, and the drain direction is from the indoor side to the outdoor side. In the external insulation structure, there are two layers of graphite polystyrene plate (100 mm thick), and the insulation effect of polystyrene plate near the outdoor side is better than that near the indoor side. The combination of anticrack mortar (5 mm thick) and paint cannot completely prevent the infiltration of rainwater, but the infiltration of rainwater in the wall will be quickly discharged in a short time.

The study only measured the temperature and humidity of the outer wall, but the performance of the outer wall is far more than these two parameters, so the next research can be done in the direction of other parameters.

Data Availability

No data were used to support this study.

Conflicts of Interest

The authors declare that there are no conflicts of interest regarding the publication of this article.

References

[1] S. Xiong and X. Gao, "Application and technology of external thermal insulation system for passive ultra-low energy consumption building," *Construction Science and Technology*, vol. 11, pp. 56–60, 2018.

[2] H. Künzel, H. M. Künzel, and K. Sedlbauer, "Long-term performance of external thermal insulation systems (ETICS)," *Acta Architectura*, vol. 5, no. 1, pp. 11–24, 2006.

[3] German Institute of Passive House, *Standard for Passive Energy Saving Reconstruction and Standard for Passive*, 2015, https://passipedia.org/_media/picopen/cnuebersetzungneuer kriterien2015.pdf.

[4] 16J908-8, *Passive Low Energy Consumption Building -- Residential Building in Cold and Cold Regions*, China Planning Press, Beijing, China, 2017.

[5] G. Chen, Y. Liao, Y. Zeng, Z. Fu, and L. Deng, "Research status and development requirements of thermophysical property testing of materials," *China Testing*, vol. 5, pp. 13–16, 2010.
[6] L. Sun, Z. Yan, and F. Chi, "Influence of moisture characteristics of plaster layer on moisture content of external thermal insulation system of rock wool," *Journal of Xi'an University of Architecture and Technology*, vol. 50, no. 1, pp. 72–77, 2018.
[7] S. Yu, *Study on Thermal and Moist Physical Properties of Wall Materials*, Northeastern University, Shenyang, China, 2018.
[8] Z. Jia, *Study on Thermal and Moisture State Analysis of Building Envelope*, Beijing Jiaotong University, Beijing, China, 2010.
[9] S. J. Chang, S. Wi, S. G. Kang, and S. Kim, "Moisture risk assessment of cross-laminated timber walls: p," *Building and Environment*, vol. 168, Article ID 106502, 2020.
[10] J. H. Park, Y. Kang, J. Lee, S. J. D. Wi, and S. Kim, "Analysis of walls of functional gypsum board added with porous material and phase change material to improve hygrothermal performance," *Energy and Buildings*, vol. 183, pp. 803–816, 2019.
[11] L. Havinga and H. Schellen, "Applying internal insulation in post-war prefab housing: u," *Building and Environment*, vol. 144, pp. 631–647, 2018.
[12] J. Xue, *Experimental and Simulation Study on Humidity Transfer of External Insulation Wall*, Harbin Institute of Technology, Harbin, China, 2014.
[13] Y. Xia, X. Ma, Y. Zheng, and S. Li, "Research on relative humidity state in energy-saving building wall (I)," *Building Science*, vol. 31, no. 2, pp. 40–45, 2015.
[14] Y. Xia, S. Li, and C. Cheng, "Research on relative humidity state in energy-saving building wall (2)," *Building Science*, vol. 31, no. 4, pp. 73–78, 2015.
[15] R. McClung, H. Ge, J. Straube, and J. Wang, "Hygrothermal performance of cross-laminated timber wall assemblies with built-in moisture: field measurements and," *Building and Environment*, vol. 71, 2014.